Indian Journal of Radio & Space Physics
Vol. 34, February 2005, pp. 23-32

Spatial correlation function of intensity variations in the ground scintillation pattern produced by equatorial spread-F irregularities

B Engavale & A Bhattacharyya

Indian Institute of Geomagnetism, New Panvel, New Mumbai 410 218

Received 15 March 2004; accepted 6 August 2004

A theoretical model is used to relate the spatial variations found in intensity scintillation patterns formed on the ground due to scattering of VHF radio waves by equatorial ionospheric irregularities, with the spatial structure of these irregularities. As equatorial ionospheric irregularities are closely aligned with the geomagnetic field, they may be considered to constitute a two-dimensional dispersive random medium. Electron density variations, which produce refractive index irregularities in the medium, are assumed to be characterized by a power law spectrum. A numerical solution of the equation satisfied by the fourth moment of intensity variations, in the plane of the receiver, is obtained using the split step method. The S_4-index, which is the standard deviation of normalized intensity variations as well as spatial correlation function of intensity, is obtained by considering special cases of the fourth moment of intensity variations. Variation of S_4-index with the standard deviation of phase fluctuations imposed by the ionospheric irregularities is studied for irregularities with different power spectral indices. Effect of varying phase fluctuations on the 50% de-correlation scale length is also studied for weak as well as strong scintillations. The S_4-index and spatial scale lengths in the ground scintillation pattern depend on parameters like thickness and height of the irregularity layer, background plasma density, standard deviation of electron density fluctuation and irregularity power spectrum. The theoretical model is used to understand the roles of these parameters in determining the S_4-index and spatial correlation function of intensity in the ground scintillation pattern.

Keywords: Equatorial ionosphere, Ionospheric irregularities, Scintillations, Correlation function

PACS No.: 92.20 Bb; 94.20 Rr

1 Introduction

Spatial variations develop in the amplitude of VHF and higher frequency radio waves, transmitted from a geo-stationary satellite, when they propagate through the ionosphere containing electron density irregularities, resulting in a pattern of varying intensity on the ground. As the ionospheric irregularities drift across the path of the radio signal, the spatial pattern of varying intensity is converted into temporal fluctuations or scintillations and recorded by a ground receiver. The strength of scintillations is usually measured by the S_4-index, which is defined as the standard deviation of normalized intensity variations. The nature of the ground scintillation pattern formed by the propagation of radio waves through ionospheric irregularities is medium-dependent. Ambient ionospheric conditions play important roles in the evolution and structuring of ionospheric irregularities. Hence significant day-to-day variations in the structure of equatorial ionospheric irregularities are observed[1-3]. Parameters like height and thickness of the irregularity layer, strength of density fluctuations, background plasma density, irregularity power spectrum and frequency of the radio wave determine the S_4-index and the distribution of spatial scale lengths in the ground scintillation pattern. Therefore, the spatial scales and S_4-index obtained from recorded scintillation measurements contain information about the irregularities that produce the scintillations. A theoretical model is used in this paper to understand the role of the various parameters, mentioned above, in controlling the spatial structure of the ground scintillation pattern, so that information obtained from scintillation observations may be related to the characteristics of equatorial ionospheric irregularities.

The sizes of electron density irregularities, which contribute to scintillations on VHF radio waves, are in the intermediate range of a few hundred metres to a few kilometres. The fluctuations in electron density are space-time dependent and hence the ground scintillation pattern has spatial as well as temporal variations. The temporal variations in the signal intensity recorded by a receiver have contributions from the drift of the irregularities across the signal path as well as from temporal changes in the irregularity characteristics. Using classical correlation analysis, the average zonal drift of the ground scintillation pattern and the random velocity, which is a measure of temporal changes in the pattern, can be estimated. The irregularity drift speed, and hence the drift of the ground scintillation pattern, changes considerably over the course of a scintillation event[4]. Therefore, obtaining the spatial scales of intensity variations in the ground scintillation pattern from recorded scintillations is not straightforward. As far as weak scintillations are concerned, major contribution comes from irregularities with scale sizes approximately equal to the Fresnel scale. In this case, information about the size of irregularities can be obtained from the time lag for which the auto-correlation function of weak intensity scintillations decreases to 0.5, provided the drift speed of irregularities transverse to the signal path is known[5]. However, this method cannot be used when scintillations are strong. Recently, Bhattacharyya *et al.*[6] have developed a method to obtain directly the spatial correlation function of the ground scintillation pattern at any instant of time from spaced receiver scintillation observations. Using this method, a distinct seasonal difference has been found in the distribution of spatial scale lengths of ground scintillation patterns produced at Ancon, a station near the dip equator, by equatorial spread-F (ESF) irregularities[6]. A theoretical model is required to interpret the observed variations in the spatial structure of the ground scintillation pattern in terms of seasonal variations in the evolution of ESF irregularities.

2 Theoretical model

Space-time dependent electron density fluctuations $\Delta N(\vec{r},t)$, which characterize ionospheric irregularities, give rise to space-time dependent fluctuations in the refractive index as

$$\Delta n(\vec{r},t) = -\frac{\lambda^2}{2\pi} r_e \Delta N(\vec{r},t) \qquad \dots (1)$$

where λ is the wavelength of the incident radio wave and r_e the classical electron radius. At a given instant of time, phase fluctuations imposed on a radio wave propagating in the z-direction assumed normal to the irregularity layer, which extends from $z=0$ to $z=L$ and is replaced by a single phase-changing screen, are a function of the transverse spatial coordinate $\vec{\rho}=(x,y)$ only[5], i.e.

$$\Delta\phi(\vec{\rho}) = \frac{2\pi}{\lambda}\int_0^L \Delta n(\vec{\rho},z)\mathrm{d}z = -\lambda r_e \int_0^L \Delta N(\vec{\rho},z)\mathrm{d}z \qquad \dots (2)$$

Information about the spatial structure of the irregularities in the x-y plane is contained in the covariance function of these phase fluctuations as

$$B_{\Delta\phi}(\vec{\rho}) = \langle \Delta\phi(\vec{\rho}_1)\Delta\phi(\vec{\rho}_2)\rangle = \lambda^2 r_e^2 B_{\Delta N_T}(\vec{\rho}) \qquad \dots (3)$$

where, $\vec{\rho}=\vec{\rho}_1-\vec{\rho}_2$, and $B_{\Delta N_T}(\vec{\rho})$ is the covariance function of fluctuations in total electron content along the signal path.

As equatorial ionospheric irregularities are very closely aligned with the geomagnetic field, which is assumed to be in the y-direction, fluctuations in the total electron content and, hence $B_{\Delta\phi}$, are a function of the x-coordinate only. The standard deviation, σ_ϕ, of phase fluctuations is obtained from

$$\sigma_\phi^2 = B_{\Delta\phi}(0) = \lambda^2 r_e^2 B_{\Delta N_T}(0) = \lambda^2 r_e^2 2\pi L \int_{-\infty}^{+\infty} \Phi_{\Delta N}(q_x, 0)\mathrm{d}q_x \qquad \dots (4)$$

where $\Phi_{\Delta N}(q_x,q_z)$ is a two-dimensional power spectrum of the geomagnetic field-aligned equatorial ionospheric irregularities. The incident plane wave is considered to have unit amplitude. If the irregularity layer is sufficiently thin, the incident radio wave acquires complex amplitude (different from unity), at the bottom of the irregularity layer, which imposes only phase perturbations on the wave. The complex amplitude changes during further propagation of the wave in free space, and this results in the formation of a diffraction pattern in the plane of the receiver. It is assumed that receivers are placed in the plane $z=z_R$. If $E(x,z)$ is a component of the wave electric field at a point (x,z), for a plane wave propagating in the z-direction, the complex amplitude, $u(x,z)$, of the wave field is defined by

$$E(x,z) = u(x,z)\exp[-ikz] \qquad \dots (5)$$

where $k=2\pi/\lambda$ is the signal wave number. Fourth moment of the complex amplitude of the wave field in a constant z-plane is defined as

$$\Gamma_4(x_1,x_2,x_3,x_4,z) = \langle u(x_1,z)\, u(x_2,z)\, u^*(x_3,z)\, u^*(x_4,z)\rangle \qquad \dots (6)$$

The one-dimensional spatial covariance function of intensity variations in a constant z-plane is given by

$$B_I(x) = \langle I(x_1,z) I(x_2,z)\rangle \qquad \dots (7)$$

where the angular brackets denote an ensemble average, $x = x_1 - x_2$ is the spatial lag, and in terms of the complex amplitude, the intensity I is

$$I(x,z) = u^*(x,z)\, u(x,z) \qquad \dots (8)$$

The S_4-index, which is generally used as a measure of the strength of intensity scintillations, is defined by

$$S_4^2 = \frac{\langle I^2\rangle - \langle I\rangle^2}{\langle I\rangle^2} \qquad \dots (9)$$

Therefore, the intensity correlation function in the plane of the receiver as well as the S_4-index may be derived from special cases of the fourth moment of the complex amplitude of the wave.

The coherence scale d_I, which is the spatial lag at which the intensity spatial correlation function falls to 50% of it's maximum value of unity at $x = 0$, gives an estimate of the dominant spatial scale length present in the ground scintillation pattern. In order to calculate d_I and the S_4 index, the fourth moment, Γ_4, of complex amplitude in the plane $z = z_R$, where the receivers are located, is calculated by solving the equation satisfied by Γ_4. Since the size of the irregularities is much greater than the wavelength of the radio wave signal under consideration, the waves are essentially scattered in the forward direction. For three-dimensional irregularities, the moment equation satisfied by Γ_4 is given by[7]

$$\begin{aligned}\frac{\partial}{\partial z}\Gamma_4(\vec{\rho}_1,\vec{\rho}_2,\vec{\rho}_3,\vec{\rho}_4,z) &= \frac{-i}{2k}\left[\left(\nabla_1^2 - \nabla_3^2\right) + \left(\nabla_2^2 - \nabla_4^2\right)\right]\Gamma_4 \\ &-\lambda^2 r_e^2\left[2A_{\Delta N}(0) - A_{\Delta N}(\vec{\rho}_1 - \vec{\rho}_3)\right. \\ &- A_{\Delta N}(\vec{\rho}_2 - \vec{\rho}_4) + A_{\Delta N}(\vec{\rho}_1 - \vec{\rho}_2) \\ &\left.- A_{\Delta N}(\vec{\rho}_1 - \vec{\rho}_4) - A_{\Delta N}(\vec{\rho}_2 - \vec{\rho}_3) + A_{\Delta N}(\vec{\rho}_3 - \vec{\rho}_4)\right]\Gamma_4\end{aligned} \qquad \dots (10)$$

where r_e is the classical electron radius and $A_{\Delta N}(\vec{\rho})$ the integrated spatial covariance function for electron density variations defined by:

$$A_{\Delta N}(\vec{\rho}) = \int_{-\infty}^{+\infty} B_{\Delta N}(\vec{\rho},z)\,\mathrm{d}z \qquad \dots (11)$$

For two-dimensional irregularities, with no density variations in the y-direction, $A_{\Delta N}$ is a function of the x-coordinate alone. In order to simplify Eq. (10), a transformation is carried out to a set of new variables ξ_1, ξ_2, X, x and ς as

$$\begin{aligned} X &= \frac{k_0}{4}(x_1 + x_2 + x_3 + x_4) \\ x &= k_0\left[(x_1 + x_2) - (x_3 + x_4)\right] \\ \xi_1 &= \frac{k_0}{2}\left[(x_1 + x_3) - (x_2 + x_4)\right] \\ \xi_2 &= \frac{k_0}{2}\left[(x_1 - x_3) - (x_2 - x_4)\right] \\ \varsigma &= \frac{k_0^2 z}{k}\end{aligned} \qquad \dots (12)$$

with $k_0 = 2\pi/R_0$, where R_0 is a characteristic scale size of the irregularities, which will be defined later. In terms of these variables, Eq. (10) assumes the form

$$\frac{\partial\Gamma_4}{\partial\varsigma} = \left[-i\frac{\partial^2}{\partial x\partial X} - i\frac{\partial^2}{\partial\xi_1\partial\xi_2} - \frac{1}{2\varsigma_L}F(x,\xi_1,\xi_2)\right]\Gamma_4 \qquad \dots (13)$$

where

$$\varsigma_L = k_0^2\, L/k$$

and

$$\begin{aligned}\frac{1}{2\varsigma_L}F(x,\xi_1,\xi_2) &= \lambda^2 r_e^2 \\ &\left[2A_{\Delta N}(0) - A_{\Delta N}(x_1 - x_3) - A_{\Delta N}(x_2 - x_4) + A_{\Delta N}(x_1 - x_2)\right. \\ &\left.- A_{\Delta N}(x_1 - x_4) - A_{\Delta N}(x_2 - x_3) + A_{\Delta N}(x_3 - x_4)\right].\end{aligned} \qquad \dots (14)$$

Here, F is independent of X, because ΔN is assumed to be a homogeneous random field, so that its covariance function can only depend on spatial lag and not on the coordinates of a point in space. The spatial covariance function of intensity defined by Eq. (7) is obtained as a special case of Γ_4, when $x_1 = x_3$ and $x_2 = x_4$. In this case $x=0$, and Γ_4 is only a function of ξ_1, ξ_2 and ς, and satisfies the equation

$$\frac{\partial \Gamma_4}{\partial \varsigma} = \left[-i \frac{\partial^2}{\partial \xi_1 \partial \xi_2} - \frac{1}{2\varsigma_L} F(\xi_1, \xi_2) \right] \Gamma_4 \qquad \ldots (15)$$

Equation (15) is solved using the 'split step' method developed by Bhattacharyya and Yeh[8]. In this method, the random medium of thickness L is divided into a number of phase screens, separated by diffraction layers. When a radio wave enters this random medium and encounters the first phase screen, the wave phase gets modulated. This modulated wave front propagates through the adjacent free-space layer, forming a diffraction pattern at the next phase screen, which again modulates the phase. In this way, phase modulations and propagation effects are imposed on the wave at and between phase screens, respectively, during the course of propagation through the random medium. When the modulated wave front finally emerges from the last phase screen and approaches the ground, only free-space propagation effects take place and a diffraction pattern is formed on the ground. In the 'split step' method, the solution of Γ_4 at $N+1^{\text{th}}$ phase screen is obtained from the solution of Γ_4 at N^{th} phase screen to finally calculate Γ_4 in the plane of the receiver.

Equatorial ionospheric irregularities generated due to plasma instabilities in post-sunset hours are usually characterized by a power law spectrum with different spectral indices under different conditions[9]. In the dip-equatorial region, where the earth's magnetic field is horizontal and nearly northward, irregularities are usually elongated along the field lines and, therefore, as noted earlier, a two-dimensional model of the irregularities may be used. A two-dimensional power-law spectrum with spectral index m is obtained as a special case of the general form of the three-dimensional irregularity power-law spectrum with spectral index p. A power-law irregularity spectrum is valid within some inner and outer scales. An isotropic two-dimensional irregularity spectrum with integral power-law index m, valid within an inner scale r_0 and an outer scale R_0 is of the form

$$\Phi_{\Delta N}(q) = \frac{\langle (\Delta N)^2 \rangle}{2\pi} \frac{K_{m/2}\left(r_0 \sqrt{q_0^2 + q^2}\right)}{K_{\frac{m}{2}-1}(q_0 r_0)} \frac{(q_0)^{\frac{m-2}{2}} r_0}{(q_0^2 + q^2)^{m/4}} \qquad \ldots (16)$$

where q is the irregularity wave number, q_0 the outer scale wave number given by $q_0 = 2\pi / R_0$, and K_m the modified Bessel's function of order m. For irregularity wave numbers that satisfy $r_0 << 1/q << 1/q_0$, Eq. (16) reduces to the single component power-law forms

$$\Phi_{\Delta N}(q) = \frac{\langle (\Delta N)^2 \rangle}{2\pi} \frac{1}{K_0(q_0 r_0)} \frac{1}{(q_0^2 + q^2)} \quad \text{for } m = 2 \qquad \ldots (17)$$

$$\Phi_{\Delta N}(q) = \frac{\langle (\Delta N)^2 \rangle}{2\pi} \frac{(m-2)\, q_0^{(m-2)}}{(q_0^2 + q^2)^{m/2}} \quad \text{for } m > 2. \qquad \ldots (18)$$

Occasionally, ESF irregularities have been found to follow a two-component power-law spectrum[10-14], where a break in the spectral slope occurs at the 'break scale length' R_b. In this case, the irregularity spectrum has the form

$$\Phi_{\Delta N}(q) = \frac{C_N}{(q_0^2 + q^2)^{\frac{m_1}{2}} (q_b^2 + q^2)^{\frac{(m_2 - m_1)}{2}}} \qquad \ldots (19)$$

where, C_N is a normalization constant, q_b the break scale wave number given by $q_b = 2\pi / r_b$ ($R_b < R_0$) and m_1 (m_2) the low (high) wave number two-dimensional power-law indices, respectively. The normalization constant C_N depends on the indices m_1 and m_2. For $m_1 = 2$ and $m_2 = 4$, C_N is given by

$$C_N = \frac{\langle (\Delta N)^2 \rangle}{2\pi} \frac{(q_b^2 - q_0^2)}{\ln(q_b / q_0)} \qquad \ldots (20)$$

The first step in the calculation of Γ_4 by solving Eq. (15) for realistic irregularity characteristics is to derive an expression for $A_{\Delta N}(x)$ in terms of the observable power spectrum $\Phi_{\Delta N}(\vec{q})$ of density variations in the ionospheric irregularities. Since $\Phi_{\Delta N}(\vec{q})$ is the Fourier transform of $B_{\Delta N}(x,z)$, it is seen from Eq. (11) that $A_{\Delta N}(x)$ may be written as

$$A_{\Delta N}(x) = 2\pi \int_{-\infty}^{\infty} \Phi_{\Delta N}(q_x, 0) e^{iq_x x} \, dq_x \qquad \ldots (21)$$

This yields the following forms for $A_{\Delta N}(x)$ for the different irregularity power spectra considered above:

(a) $m=2$

$$A_{\Delta N}(x) = \frac{\pi\langle(\Delta N)^2\rangle}{K_0(q_0 r_0)} \frac{1}{q_0} \exp\left[-q_0\sqrt{r_0^2+x^2}\right]$$

(b) $m=3$

$$A_{\Delta N}(x) = 2\langle(\Delta N)^2\rangle \, |x| \, K_1(q_0|x|)$$

(c) $m=4$

$$A_{\Delta N}(x) = \frac{\pi\langle(\Delta N)^2\rangle}{q_0}(1+q_0|x|)\exp[-q_0|x|]$$

(d) $m=5$

$$A_{\Delta N}(x) = 2q_0\langle(\Delta N)^2\rangle \, x^2 \, K_2(q_0|x|)$$

(e) $m_1=2$ and $m_2=4$

$$A_{\Delta N}(x) = \frac{\langle(\Delta N)^2\rangle}{\ln(q_b/q_0)} \frac{1}{q_0 q_b} \times\left[q_b \exp(-q_0|x|) - q_0 \exp(-q_b|x|)\right] \qquad \ldots (22)$$

These expressions are used in the calculation of S_4 index and the spatial covariance function of intensity for each case. It is necessary to consider different power spectra, because the irregularity spectrum changes as the irregularities evolve, and also as stated earlier, different irregularity spectra may be encountered under different conditions.

Intensity correlation function and S_4 index for a 251 MHz radio wave signal are estimated by choosing different values of the thickness of irregularity layer L, average height of the irregularity layer $H_{AVG} = z_R - L/2$, standard deviation of the normalized density fluctuation $\sigma_N = \langle(\Delta N)^2\rangle^{1/2}/N_0$, and the average background ionospheric plasma density N_0, which is represented by the corresponding plasma frequency ω_P. Usually, the observed maximum plasma density of the ionosphere corresponds to a plasma frequency of the order of 10 MHz and, therefore in the model, background plasma frequency is taken as 10 MHz. Height of the irregularity layer is assumed to vary within the range of 200-700 km. Thin irregularity layers with thickness L ~ 5-10 km, and thick layers with thickness L ~50-200 km are used in the model. Two different values of the outer scale equal to 10 km and 20 km, which are much greater than the Fresnel scale, $d_F = \sqrt{2\lambda z_R}$, have also been considered.

3 Computation of intensity correlation function and S_4-index

3.1 S_4-index

In the theoretical model, it is assumed that plane waves of unit amplitude are incident on the irregularity layer, in which case $\langle I(x,z)\rangle = \langle u(x,z)\, u^*(x,z)\rangle = 1$. Further, it is seen from Eqs (6) and (12) that at $z = z_R$, where the receivers are located

$$\langle I^2\rangle = \left\langle \left[u(x,z_R)u^*(x,z_R)\right]^2 \right\rangle = \Gamma_4(0,0,\varsigma_R) \quad \ldots (23)$$

where $\varsigma_R = k_0^2 z_R / k$. Also R_0, a characteristic scale size of the irregularities, which appeared in Eq. (12) through k_0 that was used to normalize the spatial scales, is now identified with the outer scale of the irregularity power-law spectrum. The S_4-index is now calculated as a special case of the solution for Γ_4, i.e.

$$S_4^2 = \Gamma_4(0,0,\varsigma_R) - 1 \qquad \ldots (24)$$

3.2 Intensity correlation function

The spatial correlation function, $C_I(x)$, of intensity variations in the plane of the receivers is derived from the covariance function $B_I(x)$ of intensity as follows

$$C_I(x)=\frac{\langle I(x_1,z_R)I(x_2,z_R)\rangle-\langle I\rangle^2}{\langle I^2\rangle-\langle I\rangle^2}=\frac{B_I(x)-1}{B_I(0)-1} \quad \ldots (25)$$

where $x=x_1-x_2$ and $B_I(x)=\langle I(x_1,z_R)I(x_2,z_R)\rangle$ is obtained as a special case of Γ_4 by setting $x_1=x_3$ and $x_2=x_4$, so that $\xi_2=0$. Therefore, $C_I(x)$ is given by the expression

$$C_I(x)=\frac{\Gamma_4(\xi,0,\varsigma_R)-1}{S_4^2}\text{, where } \xi=k_0x \quad \ldots (26)$$

4 Variation of S_4 with irregularity characteristics

The combined effect of thickness of the irregularity layer and irregularity strength as measured by the standard deviation of electron density fluctuation, is studied by considering the variation of S_4 with the standard deviation, σ_ϕ, of phase fluctuations imposed by the irregularity layer as a whole [Eq. (4)]. Figure 1 shows the variation of S_4-index with σ_ϕ for irregularities with power spectral indices m = 2, 3, 4 and 5 when the average height and thickness of the irregularity layer are taken as 500 km and 20 km, respectively. Figure 2 shows the variation of S_4-index with σ_ϕ for irregularities with a two-component power-law spectrum with power spectral indices m_1 = 2 and m_2 = 4, for different values of the break scale length R_b, when the average height and thickness of the irregularity layer are taken as 500 km and 20 km, respectively. It is seen that initially the S_4-index increases with increasing σ_ϕ in both Figs 1 and 2, although at different rates depending on the power spectrum of the irregularities. From Fig. 1 it is seen that the initial increase in S_4-index is most rapid for the shallowest slope. For m = 2, S_4 saturates for large values of σ_ϕ, and tends to a value of 1. On the other hand, for $m\geq 3$, S_4 attains maximum values exceeding 1 before asymptotically tending to a value of 1. Booker and MajidiAhi [15] had earlier obtained a similar result and suggested that when the irregularity power spectrum is sufficiently steep such that the irregularities with large scale-sizes dominate, then these irregularities tend to focus the radio waves to produce small scales in the ground intensity pattern

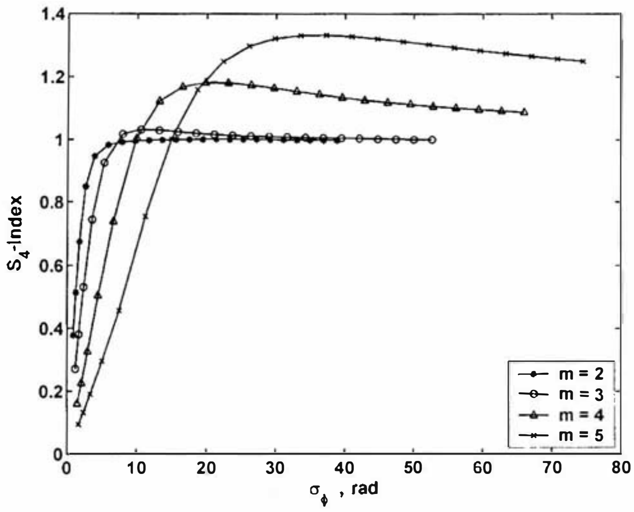

Fig. 1—S_4-index versus standard deviation, σ_ϕ, of phase fluctuations imposed by two-dimensional irregularities at an average height of 500 km, having power-law spectrum with index m = 2, 3, 4 and 5, and outer scale of 10 km (Thickness of the irregularity layer is 20 km.)

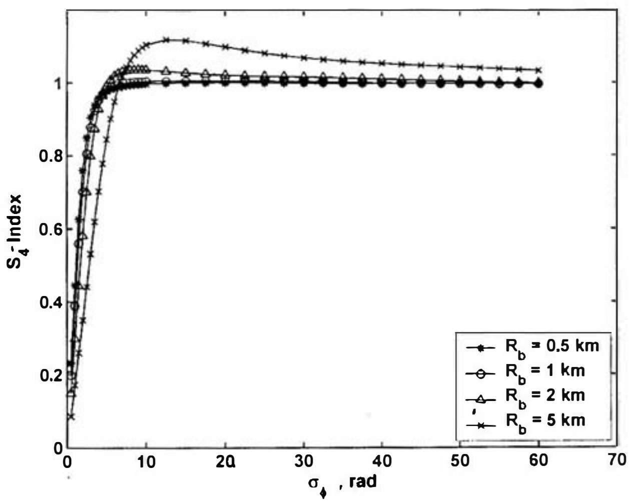

Fig. 2—S_4-index versus standard deviation, σ_ϕ, of phase fluctuations imposed by two-dimensional irregularities at an average height of 500 km, having two-component power law spectrum with indices m_1 = 2 and m_2 = 4, outer scale = 10 km, and different break scale length R_b (Thickness of the irregularity layer is 20 km.)

and values of S_4 exceed one. This tendency of large-scale irregularities to focus the incident waves is also in agreement with theoretical results obtained by Singleton[16] who considered Gaussian irregularities. The new result obtained here is for the two-component power-law irregularity spectrum shown in Fig. 2. It is seen that the break scale length must be sufficiently large for S_4 to show any focusing effects, otherwise the small-scale irregularities have enough strength to scatter the radio waves and the focusing effect is lost.

Figure 3 shows the variation of S_4-index with σ_ϕ for two different values of the average height, $H_{\text{AVG}} = z_R - L/2$, of the irregularity layer, i.e $H_{\text{AVG}} =$ 300 km and 500 km, when the irregularities have single component power-law spectra with spectral indices (i) $m = 2$ and (ii) $m = 5$. It is seen from Fig. 3 that, while there is no dependence on H_{AVG} for $m =$ 2, for the steeper slope, focusing effects set in earlier for a lower height of the irregularity layer.

5 Variation of spatial correlation function of intensity

The coherence scale d_I, which is defined by

$$C_I(x=d_I) = 0.5 \qquad \dots (27)$$

provides an estimate of the dominant scale size in the ground intensity scintillation pattern. It is seen from Fig. 4 that if only the standard deviation $\sigma_N \left(= \left\langle \Delta N^2 \right\rangle^{1/2} / N_0 \right)$ of normalized electron density fluctuations in the irregularities is changed, keeping all other irregularity characteristics the same, then the width of C_I (x) and, hence the coherence scale d_I, increases as σ_N and, therefore, σ_ϕ decreases, until d_I reaches a limiting value. This is the weak scintillation limit. On the other hand, in the variation of S_4-index with σ_ϕ, a limiting behaviour is seen for large values of σ_ϕ. In view of these limiting behaviours, dependence of d_I on the characteristics of

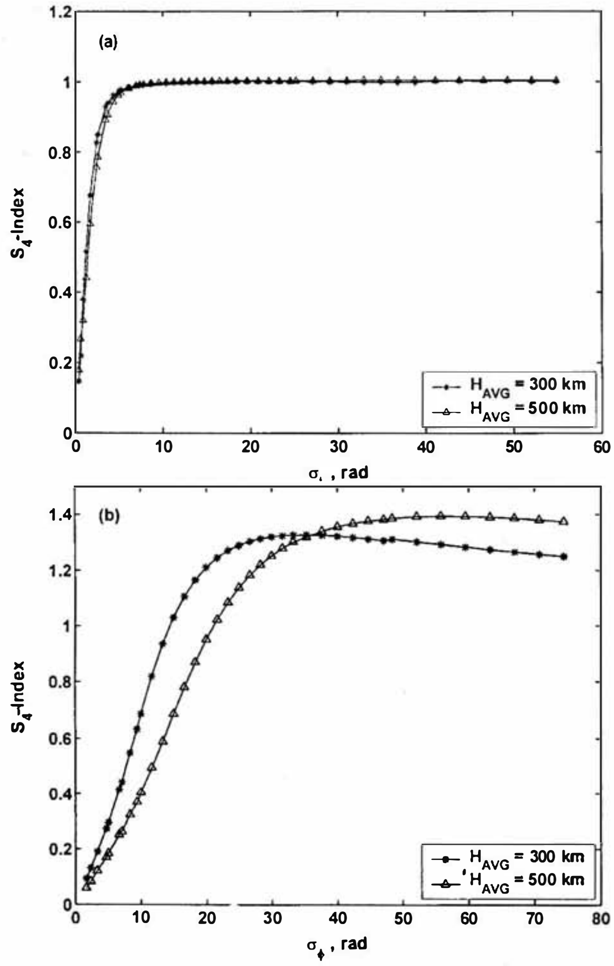

Fig. 3—Variation of S_4-index with standard deviation, σ_ϕ, of phase fluctuations imposed by two-dimensional irregularities having power-law spectrum with (a) index m = 2 and (b) index m = 5, located at average heights of 300 km and 500 km (R_0=10 km).

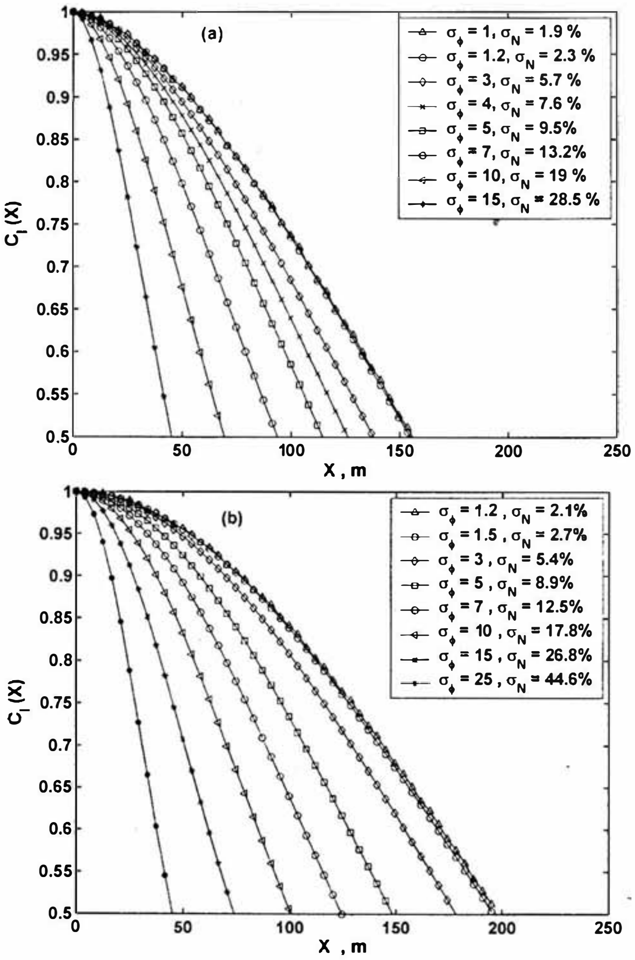

Fig. 4—Plots of C_I as a function of x for two-dimensional irregularities at an average height of 275 km, having a power-law spectrum with (a) index m=3 and (b) index m_1 = 2 and m_2 = 4 (Thickness of the irregularity layer is 50 km and R_0= 10 km).

irregularities has been studied in the two extreme cases of weak and strong scintillations.

5.1 Weak scintillations

In the following, criterion used for weak scintillations is that the S_4-index be less than 0.25. In this case, the computed coherence scales are found to vary with average height, H_{AVG}, of the irregularity layer. A plot of log (d_I) versus log (H_{AVG}) is shown in Fig. 5 for m = 2, 3, 4 and 5; and also for a two-component power-law spectrum with power spectral indices m_1 = 2 and m_2 = 4. From this plot, it is seen that d_I is proportional to $(H_{\text{AVG}})^P$, where p is dependent on the spectral index m. When scintillations are weak, major contribution to amplitude fluctuations on the ground comes from irregularities with scale sizes of the order of the Fresnel scale[5], $\left[d_F = \sqrt{2\lambda(z_R - L/2)}\right]$, and the dominant spatial scale in the ground scintillation pattern is close to the Fresnel scale. Therefore, in this case, it is expected that d_I should be nearly proportional to $\sqrt{H_{\text{AVG}}}$. Results obtained for different spectral slopes show that for m = 3 and 4, value of p is approximately equal to 0.5, as expected from the height-dependence of the Fresnel scale. For both m = 2 and 5, there is a small departure from the expected value of p. It is also to be noted that when the effective height of the irregularity layer is fixed, coherence scale d_I increases with spectral slope m. This is due to the decreasing contribution from small-scale irregularities to intensity variations on the ground, as the spectral slope increases. Figure 6 shows the intensity correlation function for m = 2 and 5 for outer scales equal to 10 km and 20 km. It is seen that irregularities with m = 2 do not show any change in coherence scale with increasing outer scale, but for irregularities with m = 5, the coherence scale changes significantly with outer scale, although the coherence scale is still found to remain proportional to $(H_{\text{AVG}})^P$ with p ~0.5. It can be concluded that as the irregularity power spectral slope becomes steeper, the spatial structure observed in the ground intensity pattern for weak scintillations is not only determined by the effective height of the irregularity layer and the

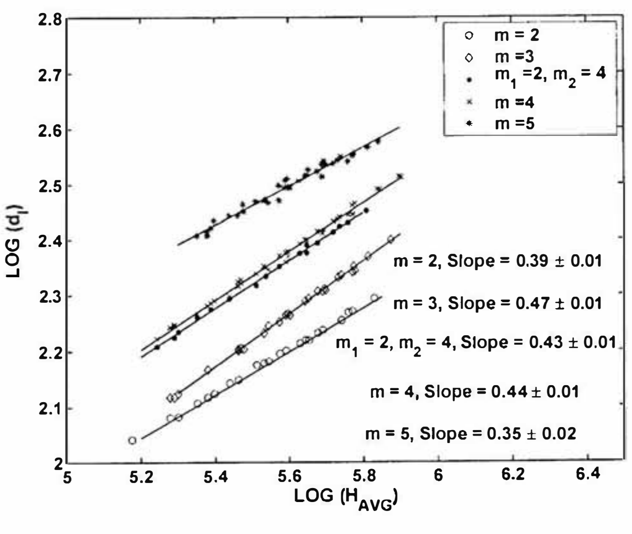

Fig. 5—Plots of log (d_I) versus log (H_{AVG}) in the weak scintillation regime for irregularities having single component power-law spectrum with m = 2, 3, 4, 5 and a two-component power law spectrum with m_1 = 2, m_2 = 4 (R_0 = 10 km)

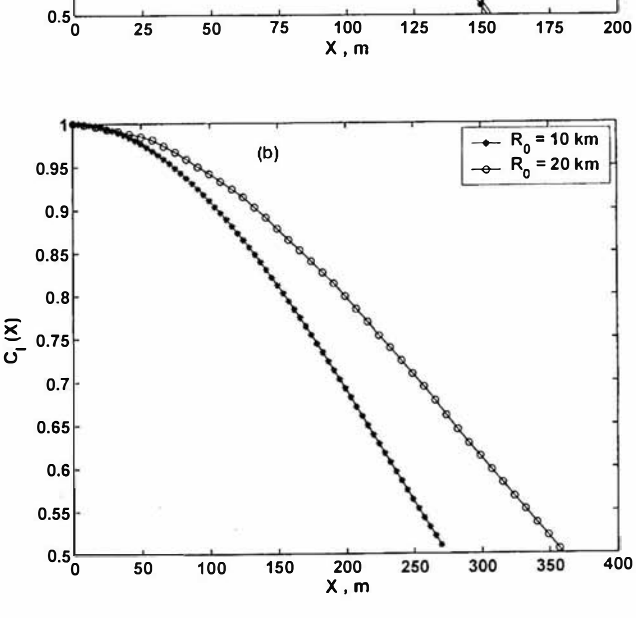

Fig. 6—Plots of $C_I(x)$ versus x for irregularities at an average height of 350 km having a single component power-law spectrum with (a) m = 2 and (b) m = 5 having outer scales of 10 km and 20 km.

irregularity power spectral index, but also begins to show a dependence on the outer scale of the power-law spectrum of the irregularities.

5.2 Strong scintillations

Scintillations are considered here to be strong when $S_4 \geq 1$. In this regime, for a fixed σ_ϕ, coherence scales become independent of the height of the irregularity layer, as seen in Fig. 7. This behaviour of d_l is entirely different from that found in the weak scintillation regime, and characterizes the strong scintillation regime. Figure 8 displays the variation of coherence scale with σ_ϕ for strong scintillations, when the slopes of single-component power-law spectra for the irregularities take on values m = 2, 3, 4 and 5, and also for a two-component power-law spectrum with power spectral indices m_1 = 2 and m_2 = 4. The coherence scale is found to vary as the inverse of σ_ϕ, irrespective of the irregularity power spectrum. This dependence also holds when the outer scale is increased to 20 km. This result is in agreement with the result obtained by Frank and Liu [10] using the asymptotic analytical form of $C_I(x)$ under the phase screen approximation[17]. The present results are valid even when the irregularity layer thickness is large. Also the dependence of coherence scales on the exact nature of the irregularity spectrum has been investigated here. In the strong scintillation regime, when σ_ϕ is kept fixed, for a single-component irregularity power spectrum, coherence scale is found

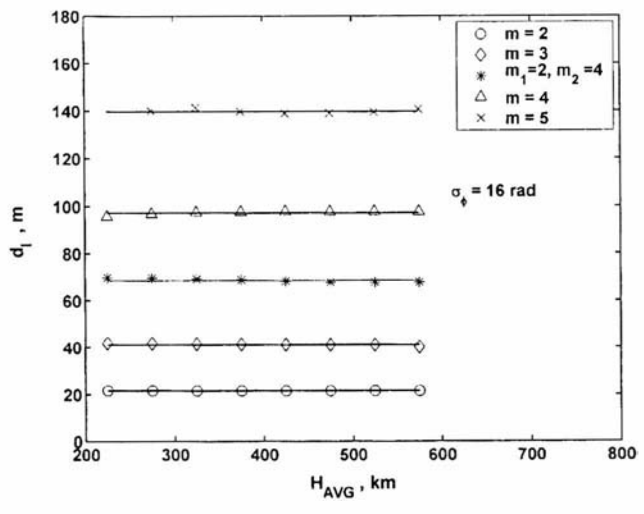

Fig. 7—Plots of d_l versus H_{AVG} in the strong scintillation regime for irregularities having a single component power-law spectrum with m = 2, 3, 4, 5 and a two-component power-law spectrum with m_1 = 2 and m_2 = 4 (R_0=10 km).

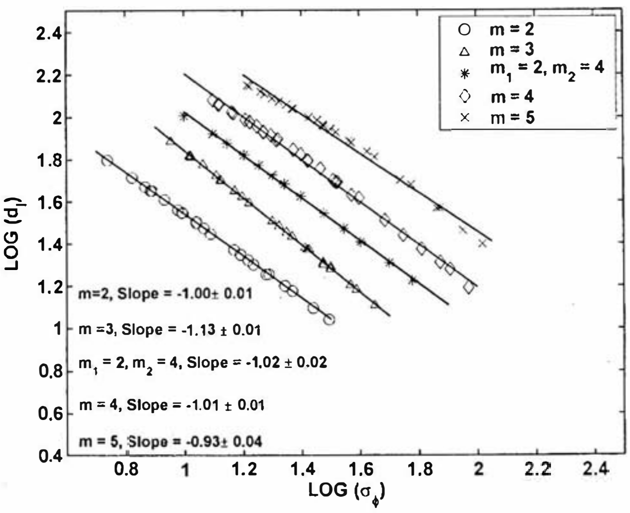

Fig. 8—Plots of log (d_l) versus log (σ_ϕ) in the strong scintillation regime for irregularities having a single component power-law spectrum with m = 2, 3, 4, 5 and a two-component power-law spectrum with m_1 = 2 and m_2 = 4 (R_0=10 km).

to be larger for steeper power spectral slopes. Also for each value of σ_ϕ in this regime, the coherence scale obtained for a two-component power-law spectrum with power spectral indices m_1 = 2 and m_2 = 4, is found to lie between the coherence scales obtained for single-component irregularity power spectra with slopes m = 3 and 4.

6 Summary and conclusions

Spatial correlation function of intensity scintillations and the S_4-index have been calculated for ionospheric irregularities with different characteristics, using a theoretical model. It is seen that large-scale irregularities give rise to focusing effects (S_4 > 1) when phase fluctuations are sufficiently large. This focusing effect is absent for irregularities with power-law spectra that have shallow slopes (m < 3), which implies a significant presence of small-scale irregularities. Also, the focusing effect seen for large-scale irregularities occurs for smaller values of σ_ϕ as the height of the irregularity layer decreases. For a two-component power-law irregularity spectrum, the break scale length must be sufficiently large for S_4 to show any focusing effects, otherwise the small-scale irregularities are effective in scattering the radio waves and the focusing effect is lost.

The dominant scale size in the ground scintillation pattern is given by the coherence scale d_l, which is the spatial lag where 50% decorrelation occurs for intensity variations in the ground pattern. As the irregularity strength and hence σ_ϕ decreases, d_l is found to attain a limiting value that is largely determined by the Fresnel scale, which depends on the height of the irregularity layer. Hence, for weak scintillations, height of the irregularity layer basically determines the dominant spatial scale in the ground scintillation pattern. However, there is also a weak dependence on the nature of the irregularity spectrum. For a fixed height of the irregularity layer, d_l is found to increase with the slope of a power-law spectrum of irregularities in the weak scintillation regime; while d_l is also seen to increase slightly with the outer scale of a power-law spectrum of irregularities as the power spectral slope increases, since the relative contribution of larger scale irregularities to the ground scintillation pattern increases in this case. In the saturated regime ($S_4 \geq 1$), coherence scale becomes independent of the height of the irregularity layer, but vary as the inverse of the standard deviation of phase fluctuations imposed by it. This in turn is determined by the r.m.s. density fluctuation in the irregularity layer and its thickness.

In the present study, no significant change was seen in either the coherence scale or S_4-index when many phase screens were replaced by a single-phase screen. This indicates that the widely used 'phase screen approximation' is good for describing scintillations under many different conditions. The results obtained here would be useful in future studies of variations in the structure of ESF irregularities due to varying ambient ionospheric conditions, using equatorial ionospheric scintillation data that extend from weak to strong scintillation regime at different stages of evolution of the irregularities.

References

1 Chakraborty S K, DasGupta A, Ray S & Banerjee S, *Radio Sci (USA)*, 34 (1999) 241.

2 Valladares C, Basu S, Groves K, Hagan M P, Hysell D, Mazzella A J (Jr.) & Sheehan R E, *J Geophys Res (USA)*, 106 (2001) 29133.

3 Devasia C V, Jyoti N, Subbarao K S V, Viswanathan K S, Tiwari D & Sridharan R, *J Atmos & Terr Phys (UK)*, 64 (2002) 1.

4 Bhattacharya A, Basu S, Groves K M, Valladares C E & Sheehan R, *Geophys Res Lett (USA)*, 28 (2001) 199.

5 Yeh K C & Liu C H, *Proc IEEE (USA)*, 70 (1982) 324.

6 Bhattacharyya A, Groves K M, Basu S, Kuenzler H, Valladares C & Sheehan R, *Radio Sci (USA)*, 38 (2003) 1004.

7 Lee L C, *J Math Phys (USA)*, 15 (1974) 1431.

8 Bhattacharyya A & Yeh K C, *Radio Sci (USA)*, 23 (1988) 791.

9 Sinha H S S, Raizada S & Misra R N, *Geophys Res Lett (USA)*, 26 (1999) 1669.

10 Franke S J & Liu C H, *Radio Sci (USA)*, 20 (1985) 403.

11 Franke S J & Liu C H, *J Geophys Res (USA)*, 88 (1983) 7075.

12 Franke S J, Liu C H & Fang D J, *Radio Sci (USA)*, 19 (1984) 695.

13 Basu S U, Basu S, Mclure J P, Hanson W B & Whitney H E, *J Geophys Res (USA)*, 88 (1983) 403.

14 Bhattacharyya A & Rastogi R G, *J Geophys Res (USA)*, 91 (1986) 11359.

15 Booker H G & MajidiAhi G, *J Atmos & Terr Phys (UK)*, 43 (1981) 1199.

16 Singleton D G, *J Atmos & Terr Phys (UK)*, 32 (1970) 187.

17 Rino C L, *Radio Sci (USA)*, 15 (1979) 1147.